U.S. Geological Survey Cooperative Agreement Award Number
Award # G18AP00007

Final Technical Report
New Lidar Mapping and Paleoseismic Characterization of the Petersen Mountain Fault Zone, North of Reno, NV

Rich D. Koehler (co-PI), Seth Dee (co-PI), and Conni De Masi

Nevada Bureau of Mines and Geology
University of Nevada, Reno
1664 N. Virginia St., MS 178
Reno, NV 89557
(775) 682-8763, fax: (775) 784-1709
http://www.nbmg.unr.edu/
rkoehler@unr.edu
sdee@unr.edu
connidemasi@nevada.unr.edu

Sept 20, 2019

Research supported by the U.S. Geological Survey (USGS), Department of Interior, under USGS award number G18AP00007. The views and conclusions contained in this document are those of the authors and should not be interpreted as representing the opinions or policies of the U.S. Geological Survey. Mention of trade names or commercial products does not constitute their endorsement by the U.S. Geological Survey.

Table of Contents

Abstract

We present results of geologic and geomorphic mapping, and paleoseismic trenching along the Petersen Mountain fault in an effort to better characterize the style and sense of deformation and paleoseismic behavior of the fault. The fault consists of two major traces (western and eastern traces) that extend between Cold Springs and Red Rock valleys north of Reno, Nevada in the northern Walker Lane. The western trace displaces colluvial, landslide, and middle to late Pleistocene alluvial fans and is associated with aligned range front saddles, linear drainages, and oversteepened range front slopes. The eastern trace of the fault is associated with a low linear bedrock ridge, right deflected stream channels, and scarps in late Pleistocene alluvial fan deposits. A paleoseismic trench was excavated across a ~3 m high scarp along the eastern trace of the fault. Stratigraphic relations exposed in the trench include disintegrated granodiorite bedrock overlain by a sandy alluvial fan in the footwall juxtaposed across a clear east dipping fault against sandy and boulder fan alluvium in the hanging wall. The stratigraphic evidence supports the occurrence of at least one late Pleistocene earthquake along the fault with a lateral sense of displacement. The combined results suggest that the Petersen Mountain fault accommodates right oblique displacement. As such, the Petersen Mountain fault accommodates part of the ~7mm/yr of dextral shear distributed across the northern Walker Lane and may represent incipient development of a strike-slip fault. Progressive development of this incipient fault may eventually link the Peavine Peak and Honey Lake faults into a more through-going fault system.

Introduction

The 25-km-long Petersen Mountain fault (PMF) bounds the eastern side of Petersen Mountain north of Reno, NV within the northern Walker Lane and extends between Cold Springs and Red Rock valleys (Figures 1 and 2). The fault is one of a series of east dipping, north-striking faults that bound basins (locally known as the North Valleys) and consists of several subparallel strands. Evidence of Quaternary deformation along the Petersen Mountain fault includes over 500 m of vertical relief along the eastern side of Petersen Mountain (a west tilted fault block), triangular facets, springs, and scarps that displace late Pleistocene alluvial surfaces. The fault is recognized as an active fault in the U.S. Geological Survey Quaternary fault and fold database and included as a source in the 2014 update of the National Seismic Hazards Model (Petersen et al., 2014).

At the latitude of the North Valleys, approximately 15-25% of the Pacific/North American plate boundary strain is accommodated east of the Sierra Nevada through a combination of normal oblique (dextral) slip on the Sierra Nevada frontal fault system and dextral slip along faults in the northern Walker Lane. Faults in the North Valleys, including the East Reno, Spanish Springs Valley, Lemon Valley, Granite Hills, Fred's Mountain, Petersen Mountain, and Last Chance faults extend between these two major tectonic elements. The North Valleys are bound on the north by the dextral Honey Lake and Warm Springs Valley faults and are truncated on the south by the Peavine Peak fault, a northwest-striking normal oblique (dextral) slip range front fault that represents the northern continuation of the Carson Range/Mount Rose fault system. Faulds et al. (2005) interpreted the North Valleys faults as a trailing imbricate fan system (e.g., Woodcock and Fisher, 1986) that accommodates oblique extension and vertical thinning. Thus, the North Valleys represent an active zone of strain transfer within the northern Walker Lane.

Geodetic studies indicate that up to 7 mm/yr of dextral shear is distributed across the northern Walker Lane and primarily accommodated along the left-stepping Pyramid Lake, Honey Lake, and Warm Springs Valley faults (Hammond et al., 2011). Geodetic studies of the North Valleys estimate that north striking faults collectively accommodate 0.9-1.2 mm/yr of extension and <0.3 mm/yr of dextral slip, with

the Petersen Mountain fault accommodating ~0.4 mm/yr of extension and 0.1 mm/yr of dextral slip (Bormann, 2013). Geologic and paleoseismic studies indicate that faults within the North Valleys all exhibit evidence of Quaternary deformation (Koehler, 2019; Dee et al., 2018; Cordy 1987; Nitchman, 19901; Nitchman and Ramelli, 1991; Soeller an Nielson, 1980; Bell, 1984), however geologic information on the timing of earthquakes, recurrence, and slip rates are sparse.

In this study, we conducted geologic, geomorphic, and fault trace mapping, paleoseismic trenching, and geochronologic studies along the Petersen Mountain fault. The objectives of these studies were to better characterize the style, sense, and paleoseismic history of deformation along the Petersen Mountain fault and evaluate its role in accommodating oblique extension in the northern Walker Lane. The results indicate that the Petersen Mountain fault is associated with multiple strands that exhibit both normal and lateral late Pleistocene deformation, in contrast to its previous characterization as a normal fault. The accommodation of lateral slip along the Petersen Mountain fault suggests that the fault may be an incipient strike-slip fault within the Walker Lane. This youthful deformation may be utilizing previous zones of weakness along previous Basin and Range normal faults.

Previous studies along the Petersen Mountain fault

The Petersen Mountain fault has been previously mapped by Dohrenwend et al. (1996), Nitchman (1991), Greene et al. (1991), Soeller and Nielsen (1980), Bell (1984), and Bonham (1969). These maps were primarily reconnaissance fault trace mapping at large scales and were compiled by Sawyer (1999) for the USGS Quaternary Fault and Fold Database (USGS, 2006). In general, these maps all describe the Petersen Mountain fault as two primary east dipping normal faults including a western trace that bounds the eastern side of Petersen Mountain and an eastern trace that extends along the eastern side of an unnamed north-trending bedrock block (herein referred to as Porcupine Ridge). The relative age of Quaternary deposits was only coarsely divided on these maps and only limited information on the age of deformation along the fault was described.

A reconnaissance study of active deformation along the Petersen Mountain fault was conducted by the Nevada Bureau of Mines and Geology in the early 1990's (Nitchman, 1991). That study identified a 2.8-m-high scarp in late Pleistocene lacustrine deposits along the southern part of the fault in Cold Springs Valley. A small hand dug trench excavated across this scarp identified two steeply east dipping fault planes and a juxtaposition of sand against warped lacustrine deltaic strata. Although the Nichman (1991) study suggests the occurrence of at least one late Pleistocene earthquake, absolute ages of the faulted deposits were not determined and comprehensive mapping of active fault traces along the length of the fault were not conducted. Nitchman (1991) also identified an ~3-m-high scarp along the central part of the fault zone but did not study it in detail. Koehler, 2019 revisited this scarp and estimated a reconnaissance vertical slip rate of 0.01-0.06 mm/yr assuming normal fault displacement and a broad age range for the displaced surface of 50-175 ka. This scarp was the focus of the paleoseismic trenching investigation conducted in this study.

Methods

Mapping of fault traces, tectonic geomorphic features, and Quaternary deposits along the Petersen Mountain fault was based on interpretation of satellite, aerial, and lidar imagery in the office and verified by field inspection. The mapping was conducted in collaboration with StateMap funded 1:24,000 scale mapping of the Granite Peak quadrangle (Dee, 2019). We utilized lidar data acquired for the Reno Carson City Urban lidar project (Washoe County) partially funded by the USGS 3DEP program (Digital Aerial Solutions, 2018). These data have an Aggregate Nominal Pulse (ANPS) spacing of 0.35 m (QL1) and 0.7 m (QL2) and were used to produce bare-earth hillshade basemaps for field mapping. The lidar data can be viewed online at http://nbmg.maps.arcgis.com/apps/webappviewer/index.html?id=2eb0b527ab8b47c8b1e09323aff14a04.

A DJI Mavic Pro drone survey was conducted at the trench site to generate low altitude images of the site. The trench was excavated, cleaned, and mapped using standard methods. A reference string grid was installed using a Spectra Precision LL300N auto level. Photos of the trench walls were captured with a Canon DG-SLR camera, and uploaded into Agisoft photogrammetry software to compile trench photomosaics. The photomosaics were printed with a 1 meter grid for field logging. A fault scarp profile was extracted from the lidar DEM's at the trench site using ArcMap. Soils developed into both the hanging wall and foot wall were described based on methods and terminology outlined in Birkeland, 1999 and Birkeland et al., 1990. Samples of soil horizons were analyzed for particle size distribution at the Desert Research Institute.

Optically stimulated luminescence (OSL) samples were collected from the trench walls for geochronologic analyses. We targeted fine quartz sand in six units distributed throughout the trench and on both sides of the fault zone. Samples were collected by tube and block sampling procedures in areas void of bioturbation to the best extent possible. The OSL field collection, lab prep and data analysis methods used in this study are based on methods described by Gray et al. (2015).

Lab prep and data analyses were completed at the Desert Research Institute in the E.L. Cord Luminescence Laboratory. A series of mechanical and chemical separations were performed under red safe-light conditions to remove unwanted minerals and grain sizes. The samples were treated with an HF etching prior to analysis. Luminescence measurements were made on an automated RISO device equipped with a radiation source, photomultiplier tube, and stimulating blue diodes. The samples were subjected to a modified SAR protocol based on Murray and Wintle (2000), which involved measuring the natural luminescence signal followed by a series of irradiations and stimulation measurements to calibrate the individual luminescence response of a 2 mm multi-grain aliquot of quartz to a given dose of radiation.

Results

Mapping observations

Our mapping efforts build upon previous reconnaissance mapping along the fault (e.g. Bell, 1984; Soeller and Nielsen, 1980; Garside, 1987) and was conducted in collaboration with 1:24,000 scale geologic mapping of the Granite Peak quadrangle related to the Nevada Bureau of Mines and Geology's (NBMG) StateMap program (Dee, 2019). Our mapping spans the entire length of the fault from Cold Springs Valley in the south to Red Rock Valley and Lee's Flat in the north and includes mapping within an intermontaine valley (drainage divide) along the central part of the fault (Figures 2 and 3). The new mapping provides details on the distribution of fault traces, tectonic geomorphic features, and Quaternary deposits. Tectonic geomorphic features and fault traces along the western and eastern strands of the Petersen Mountain fault within the Granite Springs 7.5' quadrangle are shown in Figure 3. Detailed mapping of bedrock and Quaternary deposits along the fault within the intermountain valley is on Figure 4 (Dee, 2019). A complete geologic map of the Granite Springs quadrangle is available for download from the NBMG web site.

The western trace of the fault extends generally north-south along the eastern range front of Petersen Mountain, dips steeply east (65°-87°), and is associated with several shorter splays ranging in strike from N45E to N20W (Figure 2). In the vicinity of Cold Springs Valley along the southern part of the fault, Koehler (2019) mapped the fault as a singular trace characterized by a prominent over-steepened range-front escarpment that juxtaposes bedrock against latest Pleistocene-Holocene alluvial fan deposits and basal colluvium. North of Cold Springs Valley, the western trace of the fault displaces basal colluvial slopes and landslide deposits and makes a 1.4 km right step to the western edge of the intermountain valley (drainage divide) (Dee, 2019) (Figure 4). In this area, the fault is characterized by triangular

facets, aligned springs (Blitz spring and Hillside spring), and scarps (Figure 3). Linear patches of Holocene groundwater discharge (spring) deposits locally obscure the fault scarp and are not displaced. North of the drainage divide, the western trace extends along a steep faceted range front through Little Valley to Red Rock Valley and is associated with several strands that bound a 300 m wide graben. Tectonic geomorphic features along this section include notches, range front saddles, linear drainages, over-steepened range front slopes, and displaced middle to late Pleistocene alluvial fans and landslide deposits (Figures 2 and 3).

The eastern trace of the Petersen Mountain fault extends from several kilometers south of the intermontaine valley, along the eastern side of Porcupine Ridge to Lee's Flat sub parallel to the western trace (Figure 3). The eastern trace consists of several strands distributed across a >1-km-wide zone. Individual faults of the eastern trace range in strike from N10E to N35W and dip 54° to 87° to the east-northeast. Slickensides observed on bedrock fault planes plunge from 19-21° southeast consistent with down-to-the-east dextral oblique fault motion (Figure 5). Between the drainage divide and Lee's Flat, faults associated with the eastern trace extend along Red Rock road and form a 0.5 km wide graben associated with a deeply incised linear valley. In this area, the fault displaces middle to late Pleistocene alluvial fans (Dee, 2019). Tectonic geomorphic features along the eastern trace of the fault include linear valleys, scarps, benches, and potentially right deflected stream channels (Figure 3).

Long term late-Cenozoic normal displacement across the western trace is demonstrated by the high relief of Petersen Mountain range front (>500 m) as well as the accumulation of Miocene sediments to the east that were likely deposited into a basin controlled by early displacement along the fault (Dee, 2019) (Figure 2). This is in contrast the eastern strand only bounds a small basin along a short length adjacent to Lee's flat (Figure 3). South of Lees flat the eastern strand is flanked on both sides by an elevated bedrock erosion surface that does not have a consistent sense of displacement across the fault, and commonly the elevation of the surface is equivalent on both sides. These observations in conjunction with dextral oblique kinematic data from fault surfaces, tectonic geomorphic features indicative of lateral motion, and absence of a deep continuous Quaternary basin suggest that the eastern strand may be primarily a Walker Lane structure, rather than a longer-lived Basin and Range style normal fault.

Petersen Mountain trench site

Based on our lidar evaluation and field mapping, we confirmed the presence of a ~3-m-high fault scarp along a strand of the eastern trace of the Petersen Mountain fault within the intermontaine valley (drainage divide) area (Figures 4 and 6). This scarp is the most prominent scarp identified during our reconnaissance. We excavated a trench (39.7828°N, -119.9411°W) across the scarp immediately south of a dirt road, approximately 3.5 km south of Red Rock road on BLM land which provided easy access to the site and the ability to obtain a subsurface excavation permit. Photographs of the open trench are shown in Figure 7 and photographs of the general characteristics of the site are shown in Figure 8. Geologic deposits in the vicinity of the trench site are shown in Figure 4 and a lidar hillshade map of the area is shown in Figure 6.

The scarp has a general north-south trend and cuts a late Pleistocene alluvial fan deposit (Figures 4, 8B, and 8D). Koehler (2019) previously characterized the surface cut by the scarp as a Quaternary/Tertiary pediment surface incised by active alluvial fans based on the presence of isolated low bedrock outcrops distributed across the drainage divide area west of the scarp. More detailed mapping conducted during this project (Dee, 2019, De Masi, 2019a, b) indicates that the surface is better characterized as a late Pleistocene alluvial fan based on its flat interfluve morphology and relative degree of incision (~10 m along the main active wash). The surface contains clasts of granodiorite (Kgdp) up to 1 meter in diameter.

The scarp at the trench site has been isolated from deposition since incision by east draining stream channels and Holocene alluvial fans. Apparent right-deflection of a channel is evident south of the trench in the lidar hillshade (Figures 6 and 8C). South of this apparent stream deflection the fault projects through a linear valley and across a low saddle. The stream deflections range in length from about 60 to 80 m. In the vicinity of the trench site, the eastern trace of the Petersen Mountain fault consists of at least three splays (Figure 4). North of the trench the splay we trenched splits into two splays, one that projects into Porcupine Ridge as a linear trough (Figure 8B) and another that extends along the eastern side of Porcupine ridge that is associated with scarps in late Pleistocene alluvial fans. The western trace of the Petersen Mountain fault is approximately 0.75 km west of the trench where it is associated with prominent linear scarps, aligned springs, and benches.

Trenching observations

A log of the trench exposure as well as uninterpreted and interpreted photomosaics are shown in Figure 9. Complete unit descriptions for deposits exposed in the trench are provided in Table 1. Descriptions of the soils developed into both the hanging wall and footwall surfaces are provided in Table 2.

The basal unit exposed in the footwall (Unit 6) consists of massive medium to course-grained angular sand. Microscopic analysis of hand samples of Unit 6 indicate that it includes quartz, plagioclase, orthoclase, biotite and hornblende minerals consistent with the local dioritic bedrock of Petersen Mountain that outcrops directly southwest of the trench. The rock is completely disintegrated (grussified) throughout the entire exposure and contains discontinuous oxidation stringers. Unit 6 is unconformably overlain by Unit 7, a thin medium to course grained sand with imbricated cobbles of granitic and volcanic composition up to 20 cm in diameter. A fining upward sequence of sand with trace pebbles and cobbles (Unit 8) overlies Unit 7. A well-developed soil (Units 9 and 10) is developed >80 cm into the footwall deposits and includes a prominent 23 cm thick reddish-brown sandy clay argillic horizon with high clay percent and course angular blocky structure (Figure 10).

The basal deposit in the hanging wall (Unit 1) is a poorly sorted fine to course-grained loamy sand with gravel and sub-rounded pebbles and cobbles and does not correlate with units exposed in the footwall. Unit 2 overlies Unit 1, and consists of medium to course grained sand with imbricated sub-rounded to rounded boulders that is 1.5 to 2 m thick and weakly bedded. The cobbles and boulders in Units 1 and 2 are disintegrated and have a quartz diorite composition. Unit 2 is buried by silty sand with trace cobbles (Unit 3). A weakly developed soil has developed into the hanging wall deposits and consists of loamy sand with a gray 20-cm-thick cambic B horizon with low clay percent and medium subangular blocky structure (Figure 10). Buried soils and colluvial wedges were not observed in the hanging wall deposits.

We interpret the footwall package as a bedrock strath or pediment surface overlain by sandy alluvial fan deposits. The high clay percent, red color of the argillic horizon, and depth of the soil developed in the footwall suggests a late Pleistocene age for the surface. This age is consistent with Dee (2019) who inferred a late Pleistocene age for intermediate aged (Qfi) alluvial fans distributed across the intermontaine valley and the trench site. The hanging wall package is interpreted as sand and boulder alluvial fan deposits. The low clay percent and gray color of the cambic B horizon, as well as the relatively shallow depth of development of the hanging wall soil suggests a latest Pleistocene-Holocene age for the surface.

Disintegrated bedrock Unit 6 in the footwall is juxtaposed across a steeply east-dipping well-defined fault against boulder alluvium (Unit 2) of the hanging wall (Figure 11). The relation between Unit 8 (footwall) and Unit 3 (hanging wall) across the fault is ambiguous, however the different degree of

soil development in these deposits and subtle shears suggest that they are also juxtaposed across the fault. The fault has an orientation of 335°/55°NE. A wide shear zone extends 10 m west from the main fault with faults and fractures that strike roughly north-south, dip eastward between 52° and 80°, and propagate through the disintegrated bedrock (Table 3 and Figure 12).

Clear juxtaposition of the footwall stratigraphy and soils against the compositionally different hanging wall deposits/soils indicates Quaternary displacement across the fault. Based on the lack of colluvial wedge deposits and buried soils in the hanging wall, we infer that the stratigraphic and structural relations indicate the occurrence of at least one earthquake that postdates the development of the footwall soil. Alternatively, if Units 3 and 8 represent an alluvial fan that was deposited across the surface after the most recent event, the age of displacement postdates the deposition of the boulder alluvium (Unit 2). This alternative is problematic given the distinctly different soils developed into the hanging wall and footwall, however it is possible that the footwall soil development has been influenced by the granitic bedrock beneath it contributing to its red color. Nevertheless, the juxtaposition of deposits and the wide shear zone within the footwall suggests the occurrence of at least one earthquake with a right oblique sense of displacement. This sense of motion is consistent with tectonic geomorphic observations from our mapping along the fault that are suggestive of strike-slip deformation.

Age dating of sediments

Sediment ages were determined through analyses of six OSL samples collected from the trench wall. Stratigraphic units sampled include Units 1, 2, 3, 4, and 8. The samples were analyzed at the Desert Research Institute E.L. CORD Luminescence Laboratory. Preparation of sediment samples was completed on site and analyses were conducted using two OSL/IRSL DA-20 Risø TL/OSL Readers equipped with multi-grain aliquot carousels. Quartz 180-250µm fraction size was used on 2mm multi-grain aliquot stainless steel discs. Aliquots that were over saturated were eliminated from our CAM age model, as well as those that were assigned a signal from the Risø Analyst software that failed to converge to a unique solution on the growth curve.

The OSL results are shown in Table 4. Preliminary analyses showed that all samples were near or at the luminescence saturation limit. We used the Central Age Model (CAM) of Risø Analyst. Three out of the six samples (PMF001, PMF003, andPMF006) were capable of producing an age (Table 4). Sample PMF001 was collected near the base of the sandy alluvial fan (Unit 8) stratigraphically above the disintegrated bedrock in the footwall and yielded an age of ~18 ka. Sample PMF003 was collected from the B horizon of the hanging wall soil (Unit 4) and yielded an age of ~3 ka. An age of ~20 ka was determined for sample PMF006 from the sandy alluvial fan (Unit 3) stratigraphically above the boulder alluvium (Unit 2) in the hanging wall.

Three samples (PMF002, PMF004, and PMF005) exceeded the lab's capabilities of registering a datable signal with our SAR protocol, and therefore could not produce a true representable age of the quartz grains. The lack of acceptable aliquots contributes towards age estimates that are younger than the actual age of the deposit. The ages associated with these samples are currently being re-evaluated. However, the initial analyses indicate a minimum age of ~27 ka for sample PMF002 collected from the basal sandy alluvium (Unit 1) in the hanging wall. Minimum ages of ~28 ka and 32 ka were determined for samples PMF004 and PMF005 collected from the boulder alluvium (Unit 2) in the hanging wall.

The temporal accuracy of ages determined by OSL analysis is limited by the effects of oversaturation, partial bleaching, depth penetration of cosmic rays, and bioturbation/mixing among other factors. Although the ages determined from the base of the hanging wall package (PMF002, PMF004, and PMF005) are problematic due to sample oversaturation issues they are generally older than the

stratigraphically higher samples (PMF001, PMF003, andPMF006) and loosely in stratigraphic order. We infer that the ages determined from the base of the hanging wall package may be underestimated by several ten's of thousands of years. The extremely young age for sample PMF003 (~3 ka) likely reflects partial bleaching related to mixing in the pedoturbation zone.

The approximately 20 ka age determined for the sandy alluvial deposits near the surface (but beneath the pedoturbation zone) in both the footwall and hanging wall suggests a late Pleistocene age for the surfaces. This age is consistent albeit on the younger side with ages determined elsewhere for intermediate Qfi alluvial fan deposits in the region.

Table 1. Unit descriptions for stratigraphic deposits exposed in the trench.

Unit	Description
1	Fine to course grained loamy sand with gravel to pebbles, dark tan to yellow-brown, massive, clasts are weathered granite consistent with a diorite composition (~20% quartz, 40% feldspar, and ~40% biotite and hornblende mafic minerals) (sandy alluvium).
2	Fine to course grained sand with subrounded to rounded cobbles and boulders, tan-brown, weakly bedded, clasts are imbricated, boulders are subrounded to rounded and up to 1 m diameter, quartz diorite composition (bouldery alluvial fan).
3	Silty sand with trace cobbles, tan, sand is fine to medium grained, cobbles up to 20 cm, similar to Unit 2 but slightly finer grained (sandy alluvial fan).
4	Loamy sand, brownish-gray, sand is fine to medium grained (sandy alluvium with B-horizon soil development).
5	Loamy sand to silty sand, brownish-gray, sand is fine to medium grained (sandy alluvium mixed and aeolian silt with A-horizon soil development, similar to Unit 10).
6	Coarse sand to gravel, color ranges between gray, tan, black, and orange, grains are angular, contains discontinuous irregular, thin (2-5 cm) oxidized bands related to groundwater staining, highly fractured, massive Contains quartz, plagioclase, orthoclase, biotite and hornblende. Mineral percentages include Quartz (~25%) and feldspar (~45%), with feldspars predominantly plagioclase (~85%) consistent with the Granodiorite of Petersen Mountain (disintegrated bedrock).
7	Sand with gravel and cobbles, reddish-brown, cobbles are mixed granitic and volcanic lithologies and subrounded to subangular, matrix is medium to course grained sand (debris flow or alluvial fan deposit).
8	Medium to course grained sand with trace pebbles and cobbles, reddish brown, massive (sandy alluvial fan).
9	Fine to medium grained sand with trace pebbles and cobbles, reddish brown, massive (sandy alluvium with Bt-horizon soil development becoming sandy clay loam towards base).
10	Loamy sand to silty sand with trace pebbles and cobbles, brownish gray, massive, correlative with A-horizon developed in the hanging wall (sandy alluvium mixed and aeolian silt with A-horizon soil development, similar to Unit 5).

Table 2. Soil descriptions from the south wall of the trench.

Depth (cm)	Horizon	Description*
Hanging wall		
0-24	A	Light brown, loamy sand, 10% gravel, single grain to weak very fine granular structure, non-sticky, non-plastic, loose to very friable consistence (m and d), no clay films, abrupt wavy basal contact.
24-45	Bw	Gray brown, loamy sand, 10% gravel, moderate medium subangular blocky structure, non-sticky, non-plastic, friable (m), slightly hard (d) consistence, no clay films, clear wavy basal contact.
45-68	BCm	Light brown, loamy sand to sand, 10% gravel, moderate medium to fine subangular blocky structure, non-sticky, non-plastic, firm (m), slightly hard (d) consistence, no clay films, cemented (silica?), gradual wavy basal contact.
68-90+	C	Yellow brown, sand, 10% gravel, single grain to weak friable subangular blocky structure, non-sticky, non-plastic, firm (m), hard (d) consistence, no clay films, cemented (silica?).
Footwall		
0-6	A	Light brown, loamy sand, <10% gravel, single grain to weak fine to medium subangular blocky structure, non-sticky, non-plastic, very friable (m), loose to weakly coherent (d) consistence, no clay films, abrupt wavy basal contact.
6-14	Bw	Brown, Sandy loam, <10% gravel, moderate medium subangular blocky structure, slightly sticky, slightly plastic, friable to firm (m), slightly hard (d) consistence, no clay films, abrupt wavy basal contact.
14-37	2Bt1	Reddish brown, Sandy clay, 10% gravel, strong, medium to course angular blocky structure, sticky, plastic, extremely firm (m), extremely hard (d) consistence, many distinct clay films on ped faces, pores, and bridges, gradual wavy basal contact.
37-55	2Bt2m	Light reddish brown, sandy clay loam, 10-25% gravel, strong medium subangular blocky structure, slightly sticky, slightly plastic extremely firm (m), extremely hard (d) consistence, many distinct clay films on ped faces, pores, and bridges, cemented (slilica?), diffuse wavy basal contact.
55-80	2Bt3m	Tan brown, sandy clay loam, 10-25% gravel, strong medium subangular blocky structure, non-sticky, slightly plastic, very firm (m), very hard (d) consistence, few, faint clay films on ped faces, cemented (silica?), gradual wavy basal contact.
80-110	Cox	Tan, sand to loamy sand, 10% gravel, weak fine to medium subangular blocky structure, non-sticky, non-plastic, very friable (m), weakly coherent (d), no clay films.

*For consistence, m, moist; d, dry

Table 3. Orientations of faults and fractures exposed in the footwall of the trench.

Type	Measurement location*	Attitude
Primary fault plane	D	335 º /55 ºNE
Fracture	A	355º/62º
Fracture	B	352º/78º
Fracture	C	12º/74º
Fracture	E	348º/52º
Fracture	F	10º/70º
Fracture	G	2º/85º
Fracture	H	8º/75º
Fracture	I	356º/60º
Fracture	J	355º/80º

*location of fracture measurements are shown on trench log in Figure 9.

Table 4. Optically stimulated luminescence data from the Petersen Mountain trench. Ages associated with samples highlighted in gray are under current reevaluation in the lab.

Sample number	Trench unit	Depth (m)	Over-dispersion (%)	CAM	D_b (Gy)[b]	U (ppm)[c]	Th (ppm)[c]	K (%)[c]	External beta dose rate wet (Gy/ka)	External gamma dose rate wet (Gy/ka)	Cosmic dose rate (Gy/ka)[d]	Total dose rate (Gy/ka)[e]	Age (ka)[f]
PMF001	8	1.2	38	500.1	64.41 ± 4.45	4.58	14.00	1.15	1.69	1.46	0.26	3.41 ± 0.14	18.89 ± 1.52
PMF002	1	3.0	21	752.4	97.32 ± 12.51	3.54	14.30	1.60	1.90	1.47	0.21	3.57 ± 0.16	27.23 ± 3.71
PMF003	4	0.4	46	100.35	12.56 ± 0.586	3.54	18.05	1.72	2.06	1.67	0.32	4.05 ± 0.18	3.10 ± 0.20
PMF004	2	1.7	28	843.3	110.8 ± 13.56	3.55	13.40	1.43	1.75	1.38	0.25	3.38 ± 0.15	32.78 ± 4.26
PMF005	2	2.3	23	848.45	107.2 ± 13.01	3.95	14.25	1.71	2.02	1.54	0.23	3.79 ± 0.17	28.30 ± 3.66
PMF006	3	0.7	22	834.65	104 ± 10.55	4.65	23.60	2.05	2.56	2.14	0.28	4.98 ± 0.22	20.88 ± 2.31

[b] The error shown on the burial dose, D_b, is the error modeled with the central age model (CAM) (Galbraith et al., 1999).

[c] Insert note about how U, Th, and K are measured.

[d] Cosmic dose rates (Gy/ka) are calculated according to Prescott and Hutton (1994).

[e] Dose rates (Gy/ka) were calculated using the conversion factors of Liritzis et al. 2013 and are shown rounded to two decimal places; ages were calculated using values prior to rounding; central values are given for dose-rates and errors are incorporated into that given for the total dose-rate. Water content of 3% ± 1.5% was used for all dose rate calculations.

[f] Luminescence ages were calculated using DRACv1.2 (Durcan et al., 2015) and are expressed as thousands of years before 2015 and rounded to the nearest year. Error is 1 sigma.

Discussion

The Petersen Mountain fault has previously been characterized as a range front normal fault (Sawyer, 1999; USGS, 2006), however our detailed geologic mapping shows that the fault is a more complex zone of multiple subparallel traces with cross faults and other short stepping strands. Fault striations measured on calcified fault planes indicate down-to-the-east dextral oblique slip along the fault. Additionally, tectonic geomorphic features along the fault including linear valleys, aligned saddles, notches, and benches, springs, and scarps are consistent with a component of lateral deformation.

Stratigraphic and structural relations exposed in the trench show juxtaposition of sand and boulder alluvial fan deposits (Units 1, 2, and 3) against disintegrated bedrock and alluvial fan deposits (Units 6, 7, and 8). Soils developed into these deposits are also juxtaposed across the fault, however, clear fault planes have been obscured by soil processes. The relations suggest the occurrence of at least one earthquake characterized by oblique lateral displacement. We propose two alternative possibilities for the age of faulting. First, that faulting postdates the age of the soil developed in the footwall. The soil has characteristics similar to other late Pleistocene alluvial fans in the region. A second possibility, based on similar compositional characteristics of sandy alluvial fan deposits (Unit 8 on the footwall and Unit 3 on the hanging wall) is that these units bury the fault indicating that faulting occurred prior to their deposition but after the deposition of the boulder alluvial fan deposit (Unit 2). If true, this would suggest that the differences in soil development across the scarp may be more a reflection of parent materials and less of an indication of relative age. In either case, faulting occurred in the late Pleistocene.

Age analyses on several OSL samples performed during this project were compromised by oversaturation and may considerably underestimate the age of the deposits (re-evaluation of several samples is in progress). However, taken at face value broad constraints on the age of faulting can be inferred. In the first scenario, the alluvial fan that buries the disintegrated bedrock in the footwall (Unit 8)

is ~18 ka providing a maximum limiting age for faulting. In the second scenario, the similar age for the sandy alluvial fan deposits in the footwall (Unit 8, ~18 ka) and hanging wall (Unit 3, ~20 ka) could suggest that a sandy alluvial fan was deposited across the bedrock (footwall) and boulder alluvium (hanging wall) providing a minimum limiting age for the displacement. In this case, faulting would have occurred prior to ~20 ka and after the deposition of the boulder alluvial fan (Unit 2), which has a minimum age of ~30 ka. We prefer the second scenario, based on uncertainties of tracing the fault plane through the upper meter of the exposure, but acknowledge that the displaced deposits may be older than the OSL analyses suggest.

The geologic, geomorphic, and trench observations that indicate a component of lateral slip along the Petersen Mountain fault is consistent with its position within the northern Walker Lane, but raises several questions related to the role of the fault in the development of the Walker Lane (Figure 13). Is the Petersen Mountain fault a pre-existing Basin and Range normal fault being overprinted by Walker Lane strike-slip tectonics? Does the Petersen Mountain fault represent a horsetail splay structure associated with oblique normal faulting in a right-lateral system? Are the stepping splays of the fault system related to R and R' shears of an incipient strike-slip fault? And/or does the fault represent normal and synthetic faults of a right-lateral shear couple?

The western trace of the Petersen Mountain fault has a long history of normal displacement based on the steep relief (>500 m) along its range front and accumulation of Miocene basin sediments east of the fault. However, the western trace is associated with a topographic high (intermontaine valley and drainage divide) east of the fault, and does not have a deep Quaternary basin. The eastern trace of the fault extends across an elevated bedrock erosion surface that has similar elevation on both sides of the fault and is only associated with a small basin along a short reach of the fault at its northern end (Lee's Flat). These observations in conjunction with dextral oblique kinematic data from fault surfaces and tectonic geomorphic features and trenching observations indicative of lateral motion, suggest that the eastern trace may be primarily a Walker Lane structure, rather than a longer-lived Basin and Range style normal fault.

In the northern Walker Lane, stain accumulation measured geodetically and strain release documented in geologic studies have clearly shown that dextral slip is the primary mode of deformation (Faulds et al., 2005; Bormann, 2013; Hammond et al., 2011; Ramelli et al., 2003; 2005; Turner et al., 2008; Gold et al., 2013; Chupik, 2019). The North Valleys sit northeast of the dextral oblique Peavine Peak fault, southwest of the dextral Honey Lake and Warm Springs Valley faults, and within a major right step in the dextral fault system. Geologic studies indicate a Holocene slip rate of ~1-2 mm/yr for the Honey Lake fault (Turner et al., 2008; Wills and Borchardt, 1993). Ramelli et al. (2003; 2005) estimated a slip rate of ~1 mm/yr for the Peavine Peak fault and suggested equal components of normal and right-lateral slip. These studies suggest that dextral shear projects through the North Valleys, however accommodation of this shear has not been previously documented.

The Petersen Mountain fault is optimally oriented to transfer slip and accommodate a component of lateral deformation between the Peavine Peak and Honey Lake faults. Prominent scarps in Quaternary deposits along the southern part of the eastern trace and the central-northern part of the western trace may indicate a left step in the Petersen Mountain fault system as a whole. This would suggest that the western trace of the fault has evolved to accommodate oblique motion in the modern stress field. Lateral deformation along the Petersen Mountain fault may represent the development of a youthful dextral fault system that is overprinting a previously existing normal fault system and developing a bypass across the right step between the Sierra frontal fault system and faults in the northeastern Walker Lane. In this sense the Petersen Mountain fault may be acting to integrate the Peavine Peak and Honey Lake faults into a more throughgoing strike-slip fault.

Summary

We conducted geologic and geomorphic mapping along the Petersen Mountain fault, a 25-km-long active fault within the North Valleys area of the northern Walker Lane. The results indicate that the Petersen Mountain fault is expressed as two sub parallel traces that both exhibit subtle evidence of normal and lateral deformation including linear valleys, aligned saddles and notches, right deflected streams, scarps and triangular facets. Juxtaposition of stratigraphic units exposed in a trench across the eastern trace of the fault, the relative degree of soil development in the faulted surface, and ages of faulted deposits estimated from OSL analyses indicate the occurrence of at least one earthquake that occurred in the late Pleistocene. Reevaluation of several OSL samples (currently in progress) will hopefully place tighter constraints on the age of the last deformation. The combined observations indicate that the Petersen Mountain fault accommodates a component of dextral oblique deformation along a previously existing normal fault system. The Petersen Mountain fault provides an important kinematic link between the Sierra Nevada Frontal Fault system and faults of the northeastern Walker Lane and may represent an incipient through-going strike-slip fault. Additional paleoseismic investigations are necessary to better characterize the faults rupture parameters (slip rate, recurrence, etc.) for seismic hazards assessment.

Topics for future work

- Although our inference of lateral slip along the Petersen Mountain fault is supported by the trench relations, geologic mapping, and surficial geomorphology, additional trenching is necessary to more firmly define the lateral component of slip. Additional trench sites may be discovered by careful examination of our published quadrangle scale mapping along the fault (Dee, 2019).
- Observations on slip rate, recurrence, and slip-per event need to be better developed before accurate assessments of the seismic potential of the Petersen Mountain fault can be ascertained.
- Geophysical studies aimed evaluating basin depths along normal faults within the North Valleys may help evaluate whether the basins reflect long term Basin and Range style normal faulting or oblique extension related to a right step in a right-lateral shear zone.

Reports Published

Mapping related to this research has been published as an Open-File Report by the Nevada Bureau of Mines and Geology. Conference abstracts related to this research are listed below. A conceptual paper on the region was published during this project. An additional manuscript focused on the trenching results is currently being prepared for submittal to a peer reviewed journal and awaiting final OSL geochronology results.

- Dee, S., 2019, Preliminary geologic map of the Granite Peak quadrangle, Washoe County, Nevada: Nevada Bureau of Mines and Geology Open-File Report 19-2, 1:24,000 scale, X p.
- Koehler, R.D., 2019, Active faulting in the North Valleys region of Reno, Nevada: A distributed zone within the northern Walker Lane, Geomorphology, v. 326, p. 38-53.
- De Masi, C.*, Koehler, R.D., Dee, S., Chupik, C., Castillo, C., and Kleber, E., 2019, Paleoseismic trench investigation of the Petersen Mountain fault, North Valleys-Reno, Nevada, presented at the annual meeting of the Seismological Society of America, Seattle, WA, April 23-26, 2019.
- De Masi, C.*, Koehler, R.D., Dee, S., Chupik, C., Castillo, C., Kleber, E., and Keen-Zebert, A., 2019, New observations on the paleoseismic history and sense of slip along the Petersen Mountain fault, north western Nevada, presented at the Cordilleran section meeting of the Geological Society of America, Portland, OR, May 16, 2019.

Data Availability

The abstracts listed above are available on the conference web pages. Trench logs and GIS shapefiles of the fault trace mapping are archived on the NBMG servers at University of Nevada, Reno. The geologic map of the Granite Springs quadrangle is downloadable from the NBMG website.

Acknowledgements

This work was funded under USGS NEHRP Cooperative Agreement G18AP00007. Additional field support for De Masi was funded by the Geological Society of America Graduate Student Research Grant, and the University of Nevada Reno Graduate Student Association Graduate Student Research Grant. We appreciate field assistance during the trenching from Colin Chupik, Chris Castillo, Emily Kleber, and various groups of graduate students from UNR. Amanda Keen-Zebert of the E.L. Cord Luminesence Laboratory provided assistance in sample collection and mentored de Masi during sample preparation.

The views and conclusions contained in this Final Technical Report are those of the authors and should not be interpreted as necessarily representing the official policies, either expressed or implied, of the US Government.

References

Bell, J.W., 1984, Quaternary fault map of Nevada-Reno sheet, Nevada Bureau of Mines and Geology Map 79, 1 sheet, scale 1:250,000.

Birkeland, P.W., 1999, Soils and Geomorphology, 432 pp., Oxford University Press.

Birkeland, P.W., Machette, M.N., and Haller, K.M, 1990, Soils as a tool for applied Quaternary geology, Manual for a short course, May 30-June1, 1990, Utah Geological and Mineral Survey, Miscellaneous Publication Series.

Bormann, J., 2013. New insights into strain accumulation and release in the Central and Northern Walker Lane, Pacific-North American Plate Boundary, California and Nevada, USA. Ph.D. Dissertation. University of Nevada, Reno.

Chupik, C., 2019, Quaternary mapping and paleoseismic assessment of the Warm Springs Valley fault in the northern Walker Lane, Nevada, [M.S. thesis], University of Nevada, Reno.

Cordy, G.E., 1987, Geology and earthquake hazards Reno NE quadrangle: Nevada Bureau of Mines and Geology OpenFile Report 875, 78 p.

Dee, S., 2019, Preliminary geologic map of the Granite Peak quadrangle, Washoe County, Nevada: Nevada Bureau of Mines and Geology Open-File Report 19-2, 1:24,000 scale, X p.

Dee, S., Ramelli, A.R., and Koehler, R.D., 2018, Pilot paleoseismic investigation of faults in the North Valleys, Reno, NV, Final Technical Report, U.S. Geological Survey National Earthquake Hazards Reduction Program (Award # G16AP00060).

De Masi, C., Koehler, R.D., Dee, S., Chupik, C., Castillo, C., and Kleber, E., 2019, Paleoseismic trench investigation of the Petersen Mountain fault, North Valleys-Reno, Nevada, presented at the annual meeting of the Seismological Society of America, Seattle, WA, April 23-26, 2019.

De Masi, C.*, Koehler, R.D., Dee, S., Chupik, C., Castillo, C., Kleber, E., and Keen-Zebert, A., 2019, New observations on the paleoseismic history and sense of slip along the Petersen Mountain fault, north western Nevada, presented at the Cordilleran section meeting of the Geological Society of America, Portland, OR, May 16, 2019.

Digital Aerial Solutions, 2018, Lidar project report: NV Reno Carson City Urban: Prepared for U.S. Geological Survey, contract #16PC00044, task order #G17PD01257.

Dohrenwend, J.C., Schell, B.A., Menges, C.M., Moring, B.C., and McKittrick, M.A., 1996, Reconnaissance photogeologic map of young (Quaternary and late Tertiary) faults in Nevada, *In*: Singer, D.A. (ed.), Analysis of Nevada's metal-bearing mineral resources: Nevada Bureau of Mines and Geology Open-File Report 96-2, 1 pl., scale 1:1,000,000.

Durcan, J.A., King, G.E., and Duller, G.A.T., 2015. DRAC: Dose rate and age calculator for trapped charge dating. Quaternary Geochronology, v.28, p.54-61.

Faulds, J. E., Henry, C. D., and Hinz, N. H., 2005, Kinematics of the northern Walker Lane: An incipient transform fault along the Pacific–North American plate boundary, Geology 33, 505–508.

Galbraith, R.F., Roberts, R.G., Laslett, G.M., Yoshida, H., Olley, J.M., 1999. Optical dating of single grains of quartz from Jinmium rock shelter, northern Australia. Part I: experimental design and statistical models. Archaeometry, 41, pp. 339-364.

Garside, L.J., 1987, Reconnaissance geologic map of the Granite Peak Quadrangle, Nevada: Nevada Bureau of Mines and Geology Open-File Report 87-8, 1:24,000.

Greene, R.C., Stewart, J.H., Hohn, D.A., Hardyman, R.F., Silberling, N.J., and Sorensen, M.L., 1991, Geologic map of the Reno 1° X 2° quadrangle, Nevada and California: U.S. Geological Survey Miscellaneous Field Studies Map MF-2154-A, scale 1:250,000.

Gray, H.J., Mahan, S.A., Rittenour, T., and Nelson, M.S., 2015, Guide to luminescence dating techniques and their application for paleoseismic research, In: Lund, W.R. (ed.), 2015, Proceedings volume, Basin and Range Province Seismic Hazards Summit III, Utah Geological Survey, Miscellaneous Publication 15-5.

Gold, R.D., dePolo, C.M., Briggs, R.W., Crone, A.J., and Gosse, J., 2013, Late Quaternary slip-rate variations along the Warm Springs Valley fault system, northern Walker Lane, California- Nevada border, Bulletin of the Seismological Society of America, v. 103, no 1, p. 542-558.

Hammond, W.C., Blewitt, G., and Kreemer, C., 2011, Block modeling of crustal deformation of the northern Walker Lane and Basin and Range from GPS velocities, J. Geophys. Res. B Solid Earth Planets 116, 1-28.

Koehler, R.D., 2019, Active faulting in the North Valleys region of Reno, Nevada: A distributed zone within the northern Walker Lane, Geomorphology, v. 326, p. 38-53.

Murray, A.S., and Wintle, A.G., 2000, Luminescence dating of quartz using an improved single-aliquot regenerative-dose protocol: Radiation Measurements, v. 32, no. 1, p. 57-73.

Nitchman, S.P., 1991, Petersen Mountain fault: Nevada Bureau of Mines and Geology Preliminary Fault Evaluation Report, 3 p., scale 1:62,500.

Nitchman, S.P., and Ramelli, A.R., 1991, Freds Mountain fault: Nevada Bureau of Mines and Geology Evaluation Report, 7 p., 2 scarp profiles, scale 1:62,500.

Prescott, J.R., & Hutton, J.T. (1994). Cosmic ray contributions to dose rates for luminescence and ESR dating: large depths and long-term time variations. Radiation Measurements, 23, 497-500.

Ramelli, A. R., dePolo, C. M., and Bell, J.W., 2003, Paleoseismic studies of the Peavine Peak fault, NEHRP Technical Report, 01HQGR0167, 15 pp.

Ramelli, A. R., Bell, J.W., and dePolo, C. M., 2005, Peavine Peak fault: Another Piece of the Walker Lane Puzzle, in Lund, W.R., editor, Western States Seismic Policy Council Proceedings Volume of the Basin and Range Province Seismic-Hazards Summit II: Utah Geological Survey Miscellaneous Publication 05-2.

Sawyer, T.L., compiler, 1999, Fault number 1640, Petersen Mountain fault, *In*: Quaternary fault and fold database of the United States: U.S. Geological Survey website

Soeller, S.A., and Nielson, R.L., 1980, Geologic map, Reno NW quadrangle, Nevada Bureau of Mines and Geology Map 4Dg, scale 1:24,000.

Turner, R., Koehler, R., Briggs, R. W., and S. G. Wesnousky, 2008, Paleoseismic and slip-rate observations along the Honey Lake fault zone, northeastern California, Bulletin of the Seismological Society of America, 98, 4, 1730-1736.

U.S. Geological Survey, 2006, Quaternary fault and fold database for the United States, https://earthquake.usgs.gov/hazards/qfaults/, accessed February 2, 2019.

Figures

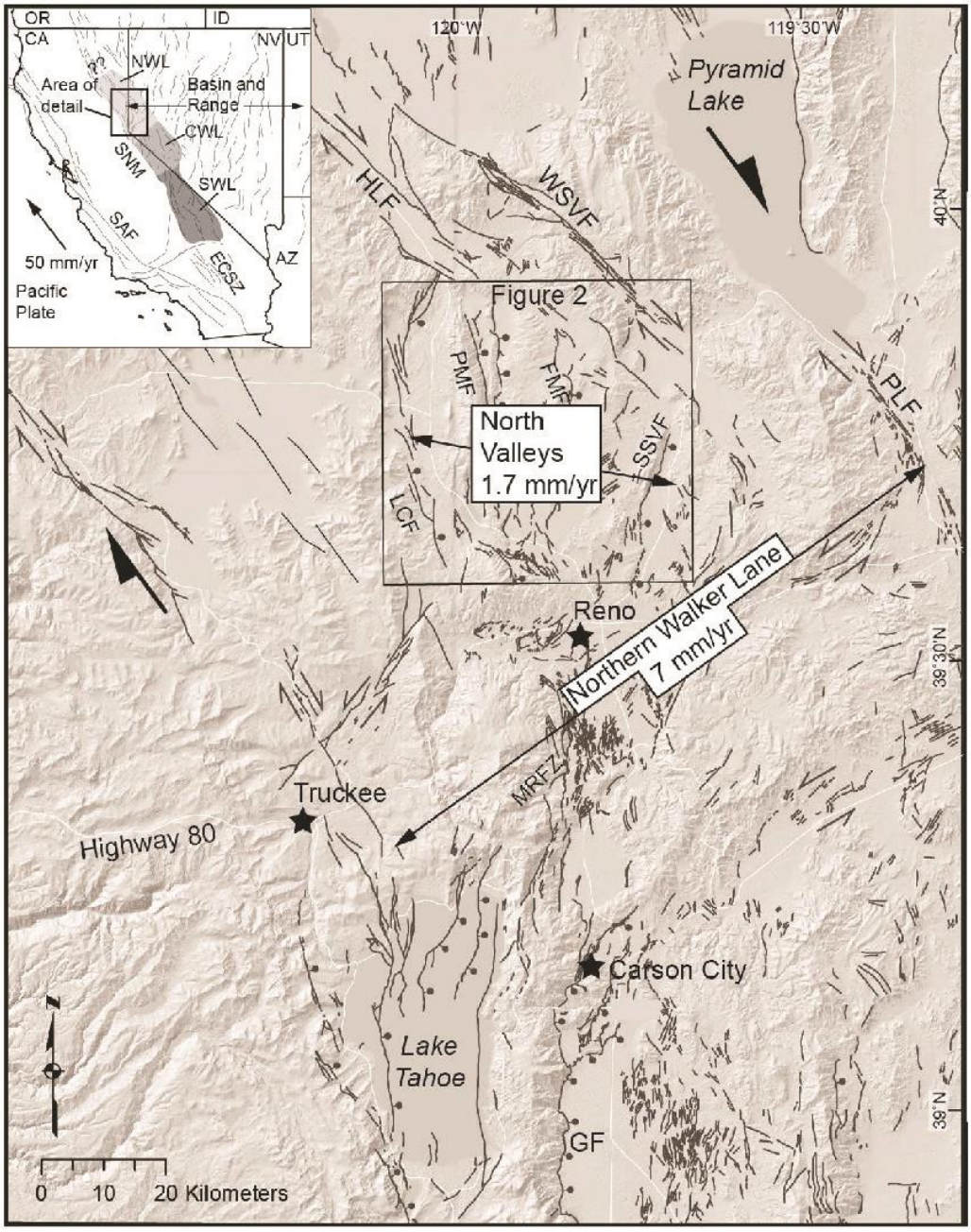

Figure 1. Regional hillshade map of the northern Walker Lane in the vicinity of Reno, NV showing major Quaternary faults (U.S. Geological Survey, 2006) and location of the North Valleys. Inset map shows the location of the study area with respect to the northern Walker Lane and the western Basin and Range Province. Geodetically determined rates of strain accumulation are shown in white boxes (Bormann, 2013). HLF, Honey Lake fault; WSVF, Warm Springs Valley fault; PLF, Pyramid Lake fault; SSVF, Spanish Springs Valley fault; FMF, Fred's Mountain fault; PMF, Petersen Mountain fault; MRFZ, Mount Rose Fault Zone; GF, Genoa fault.

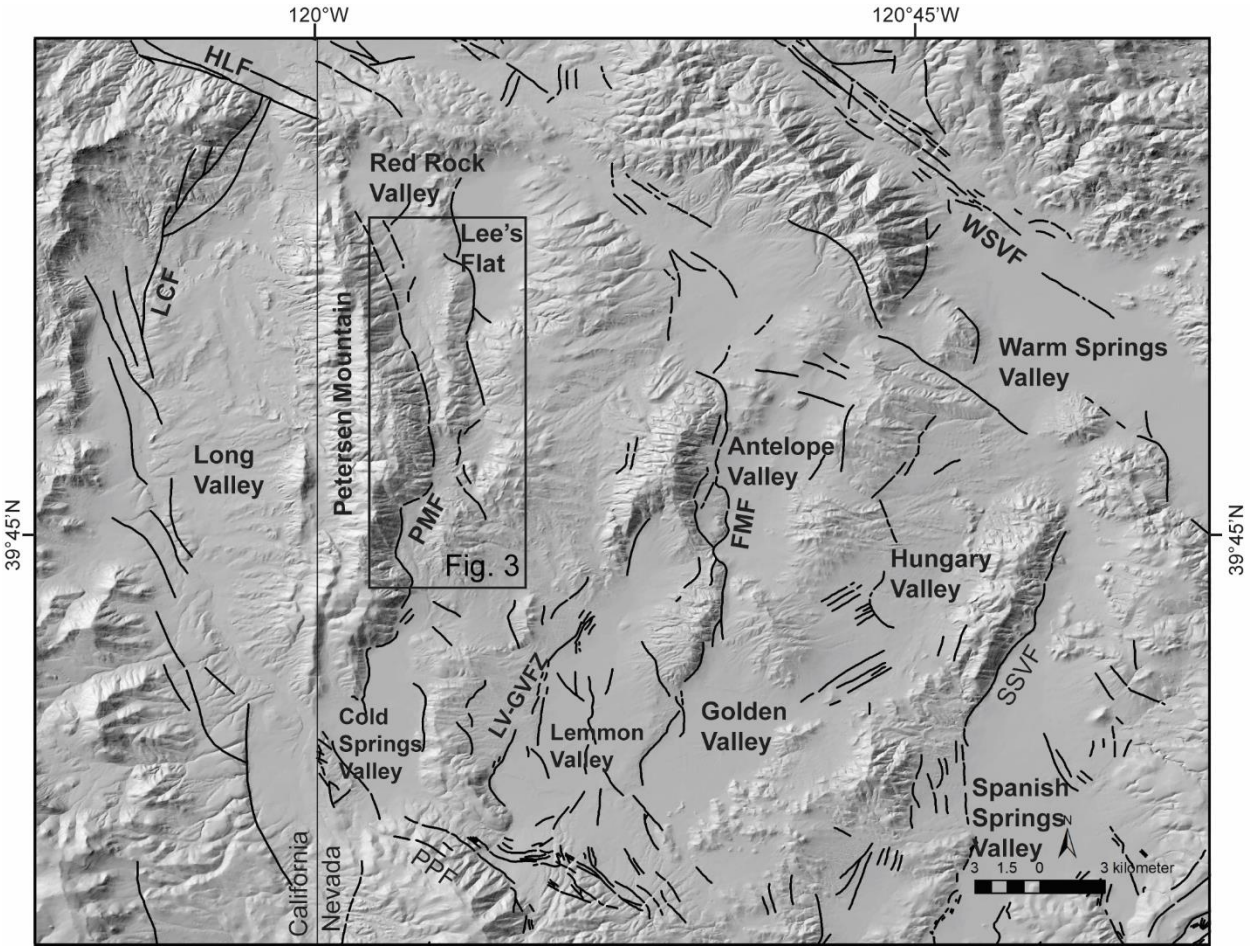

Figure 2. Hillshade map of the North Valleys including the Petersen Mountain fault. Black rectangle shows location of Figure 3. Quaternary faults (US Geological Survey, 2006). LCF, Last Chance fault; PMF, Petersen Mountain fault; PPF, Peavine Peak fault; LV-GVFZ, Lemmon Valley-Golden Valley fault zone; FMF, Fred's Mountain fault; SSVF, Spanish Springs Valley fault; HLF, Honey Lake fault; WSVF, Warm Springs Valley fault.

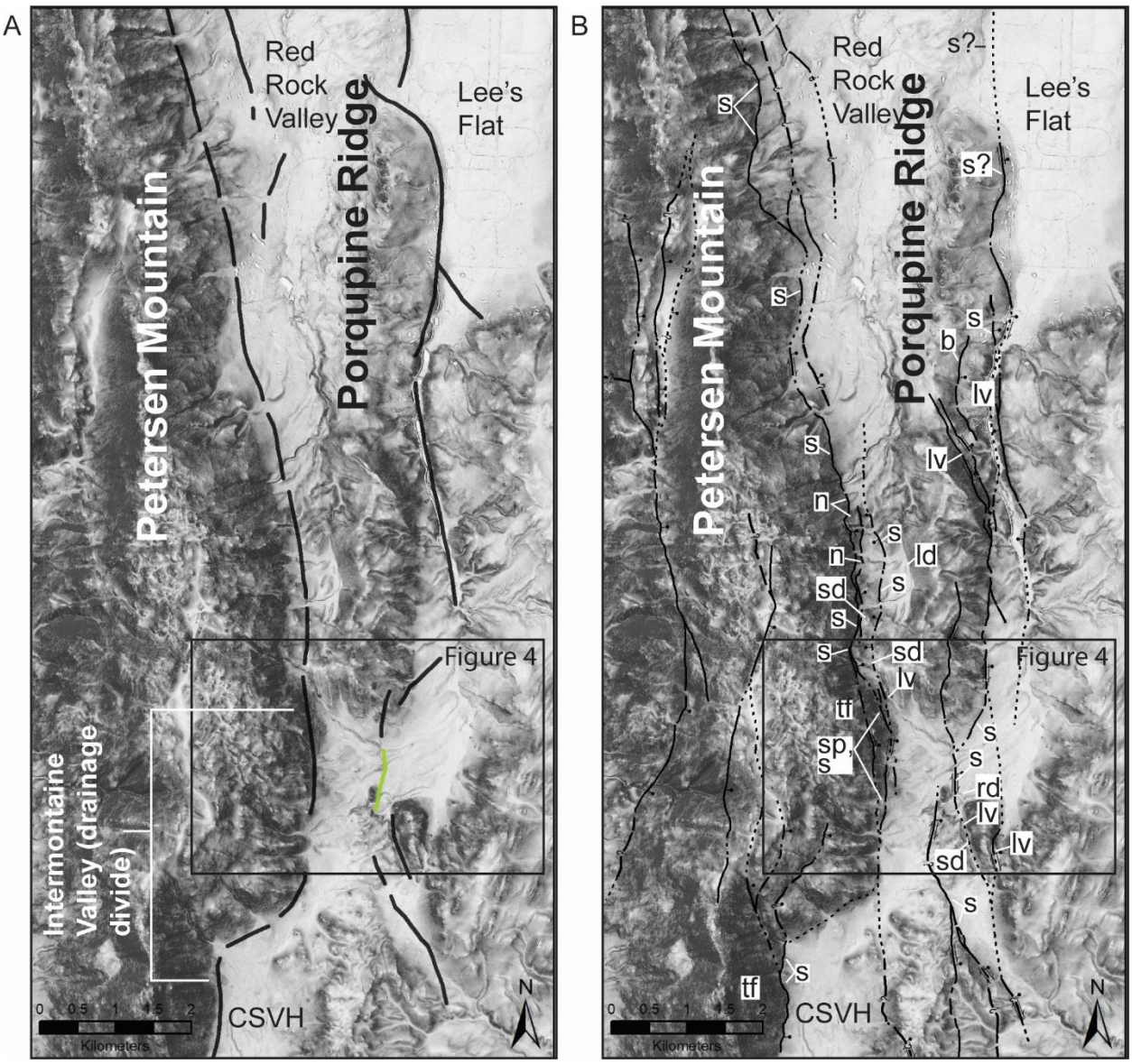

Figure 3. (A) Previous mapping showing the western and eastern traces of the Petersen Mountain fault (USGS, 2006). Age of most recent displacement shown by black lines (Quaternary, <1.6 m.y.) and green line (late Quaternary, <130,000 yrs.). (B) Lidar slope map of area in A showing major fault traces (Dee, 2019) and tectonic geomorphic features evaluated in this project. Area of detailed geologic mapping shown in Figure 4 indicated by black rectangle. Tectonic geomorphic abbreviations: s, scarp; lv, linear valley; rd, right deflection; sd, saddle; tf, triangular facet; sp, springs; b, bench; ld, linear drainage; n, notch. CSVH, headwaters of the Cold Springs Valley drainage basin.

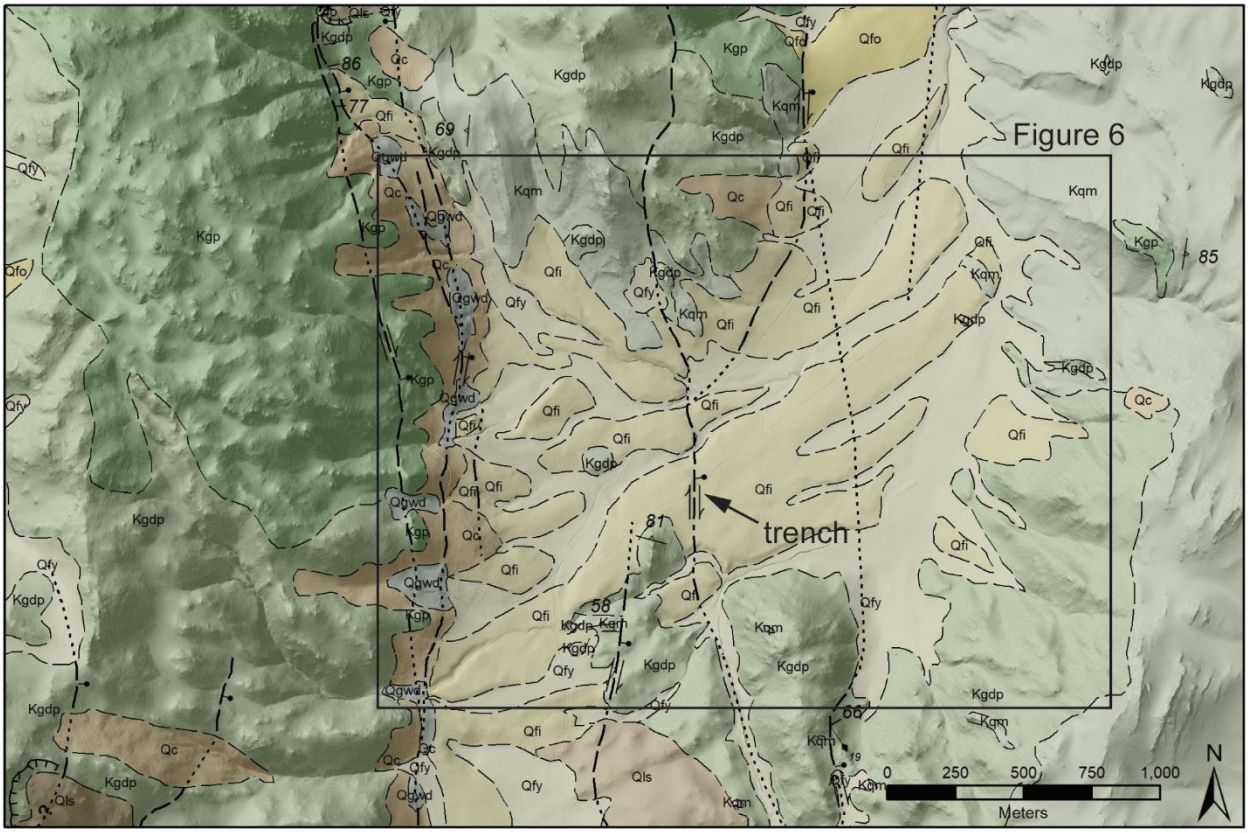

QUATERNARY DEPOSITS

- Qa — Active alluvium (Holocene)
- Qc — Colluvial deposits (Holocene)
- Qgwd — Groundwater discharge deposits (Holocene)
- Qfy — Young alluvial-fan deposits (Holocene)
- Qfi — Intermediate-age alluvial-fan deposits (late Pleistocene)
- Qfo — Older alluvial-fan deposits (middle Pleistocene)
- Qls — Landslide deposits (Holocene to late Pleistocene)

CRETACEOUS GRANITIC ROCKS

- Kqm — Quartz monzonite of Granite Peak (Cretaceous)
- Kgp — Granite of Petersen Mountain (Cretaceous)
- Kgdp — Granodiorite of Petersen Mountain (Cretaceous)
- Kgdf — Granodiorite of Freds Mountain (Cretaceous)

Contact Solid where certain, dashed where approximately located; queried if identity or existence uncertain.

Normal fault Solid where certain, dashed where approximately located, dotted where concealed; queried if idenity or existence uncertain. Showing dip; ball on downthrown side; diamond tipped arrow indicated bearing and plunge of slickenline.

Oblique-slip, right-lateral fault Solid where certain, dashed where approximately located, dotted where concealed; queried if idenity or existence uncertain. Showing dip; ball on downthrown side; diamond tipped arrow indicated bearing and plunge of slickenline.

Anticline Dashed where approximately located.

Landslide scarp Hashures point down scarp.

Figure 4. Detailed geologic mapping in the vicinity of the paleoseismic trench taken from Dee (2019). Area of Figure 6 shown by black rectangle.

Figure 5. Fault surface on the eastern strand of the Petersen Mountain fault. Fault surface is oriented 332°/66° SE with slickenside lineations on a calcified fault surface. Lineations plunge to the southeast with a 21° rake indicative of down-to-the-east dextral oblique fault motion. The fault exposure shown is located <1 km to the SE of the trench site on a parallel fault strand.

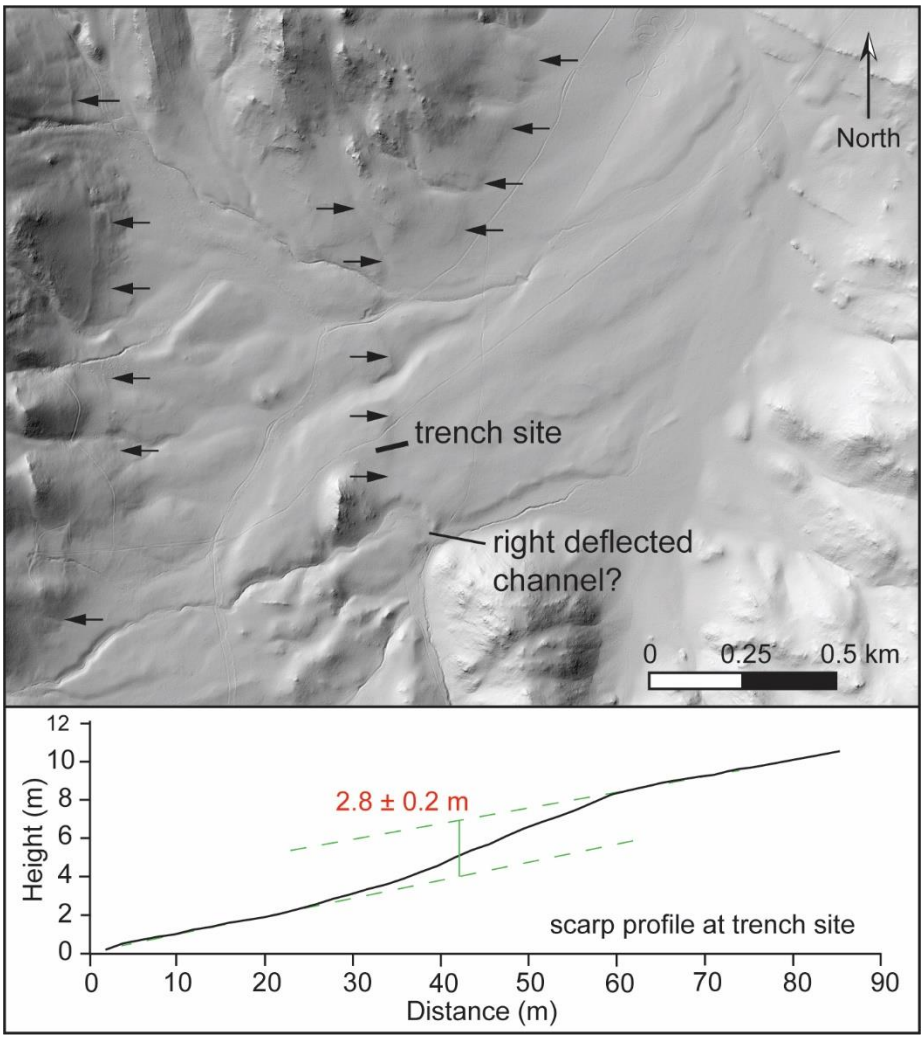

Figure 6. Lidar hillshade map of the area around the paleoseismic trench site. Black arrows indicate prominent faults. Bottom image is a fault scarp profile at the trench site showing ~3 m of vertical separation.

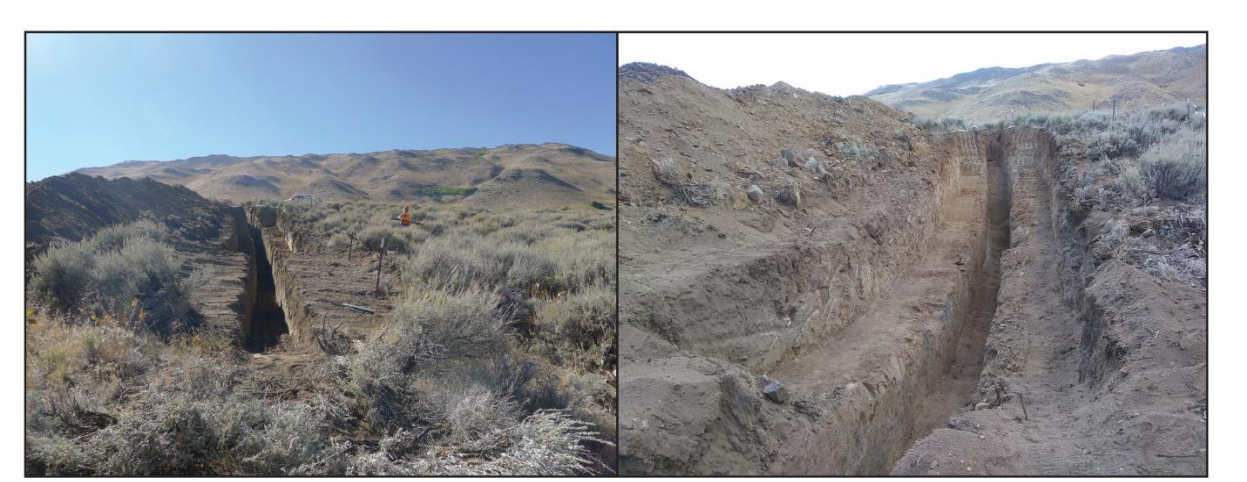

Figure 7. Photographs of the trench excavation.

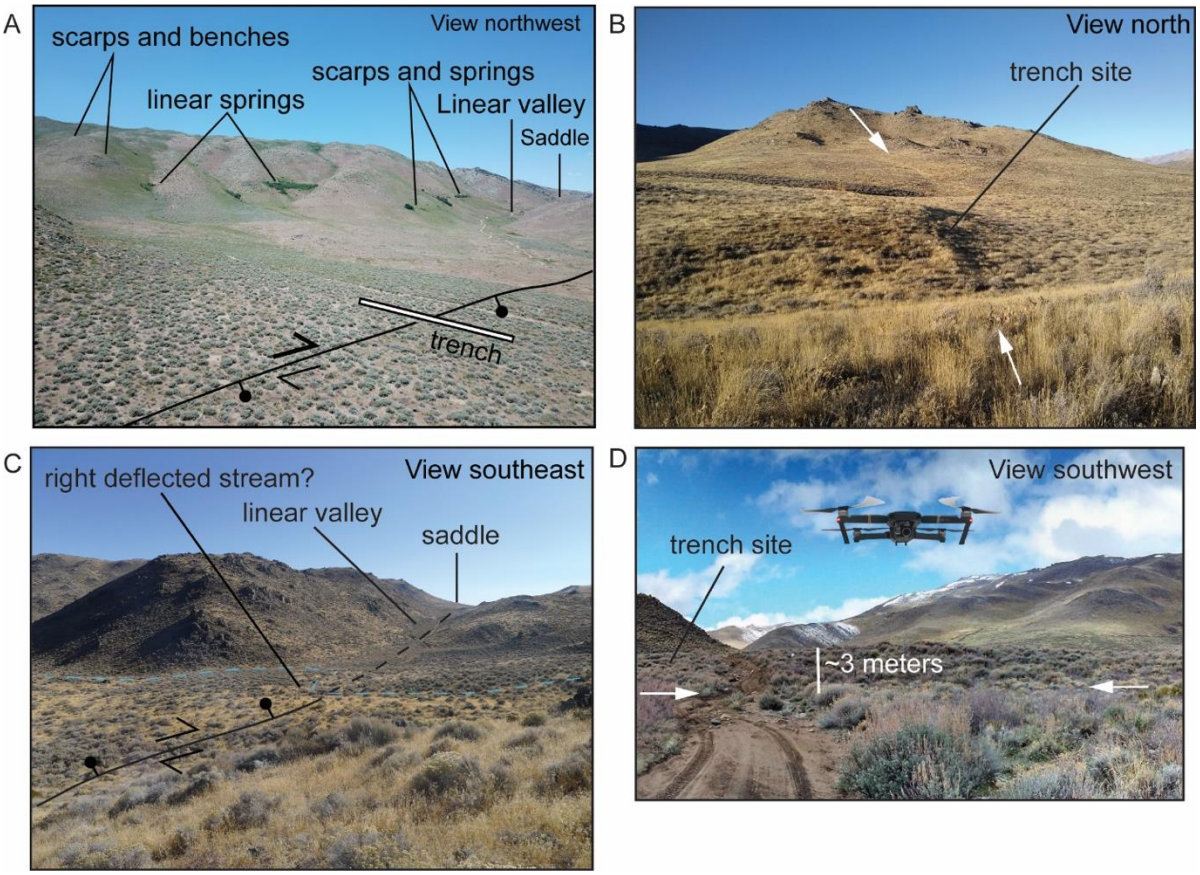

Figure 8. (A) Drone photograph of the trench site showing tectonic geomorphology along the western trace of the Petersen Mountain fault zone. (B) Photograph of the trench site along the eastern trace of the Petesen Mountain fault with the scarp shadowed by late afternoon sun. (C) Drone photograph of possible right-lateral stream deflection (dashed light blue line) located about 250 m south of the trench. (D) Close up photograph of the scarp at the trench site. Fault extends between white arrows in B and D and indicated by black line in A and C.

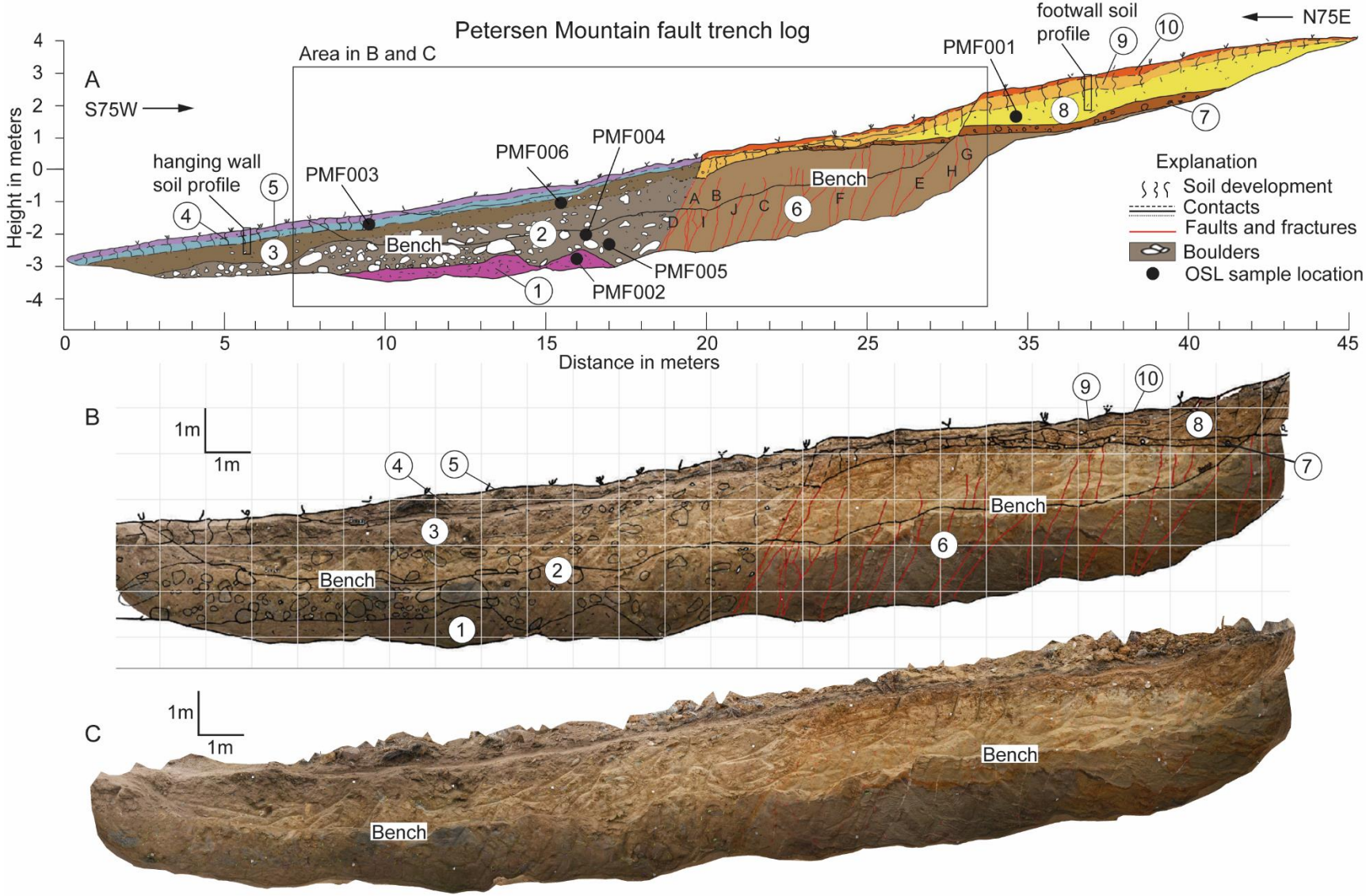

Figure 9. (A) Log of Petersen Mountain trench exposure (south wall) showing stratigraphic and structural relations. Open circles show unit numbers, solid circles are OSL samples, and letters are fracture attitude locations. (B) Interpreted photomosaic. (C) Uninterpreted photomosaic.

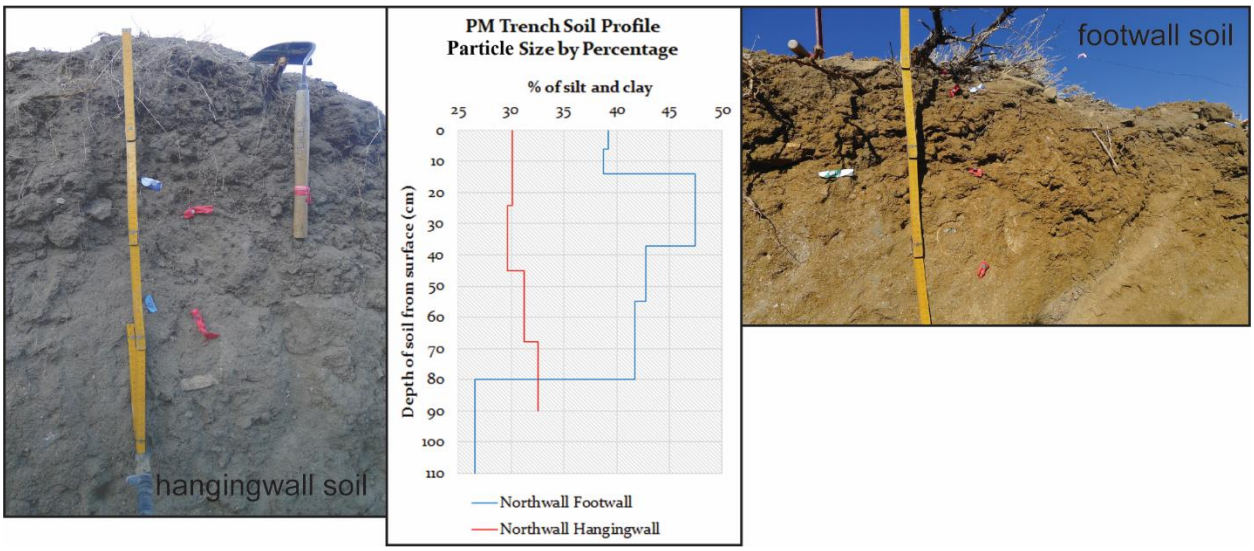

Figure 10. Photographs of soils developed into the hanging wall (left) and footwall (right). Plot in center shows percent silt and clay vs depth for both soils. The higher percentage of silt and clay and red color in the Bt-horizon in the footwall soil suggests a late Pleistocene age. In contrast, the low silt and clay percent and gray color in the Bw-horizon of the hanging wall soil suggests a latest Pleistocene-Holocene age. See Table 2 for complete soil descriptions.

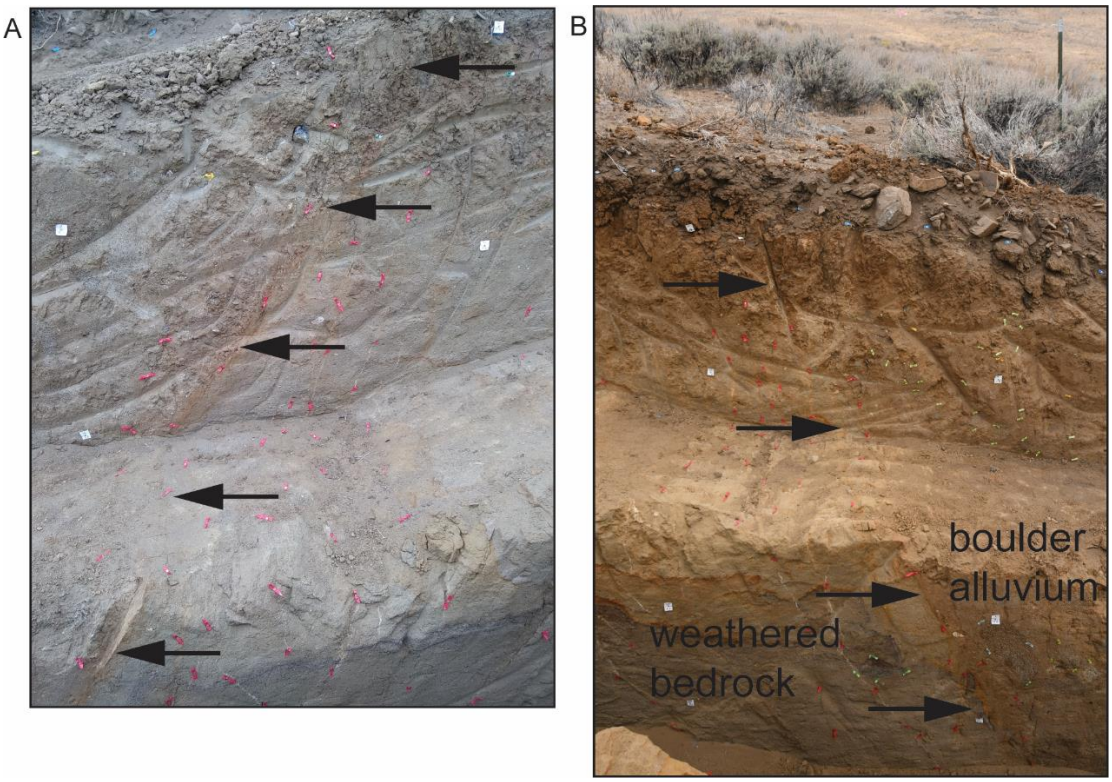

Figure 11. Close up photographs of the main fault zone in the trench exposure. (A) South wall. The fault plane is visible in the lower left of the photo where it was excavated into the trench wall. (B) North wall showing boulder alluvium juxtaposed against bedrock. Location of the main fault is shown by black arrows in both photos.

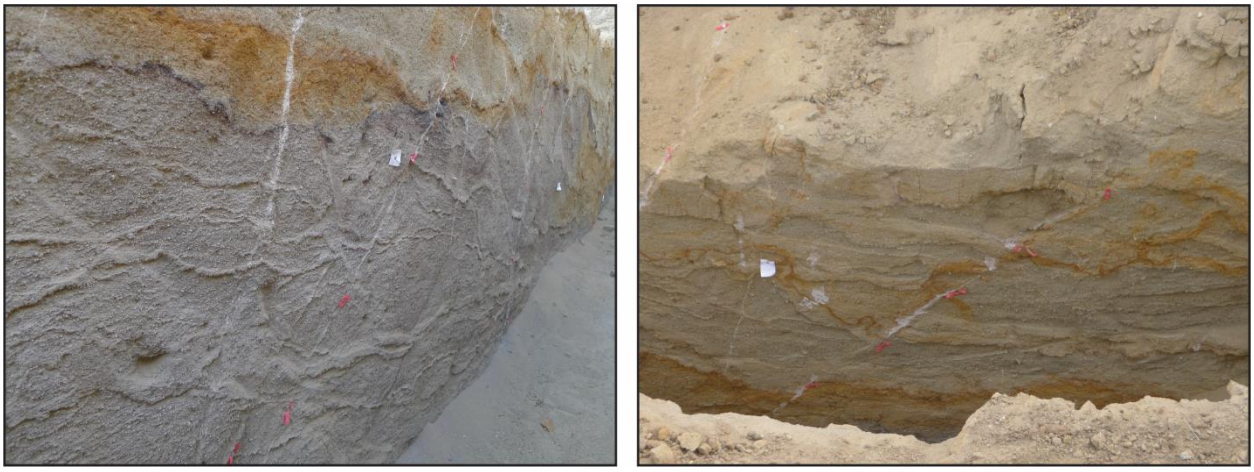

Figure 12. Photographs of fractures west of the main fault zone exposed in the south wall of the Petersen Mountain trench. Orientations of fractures are presented in Table 3.

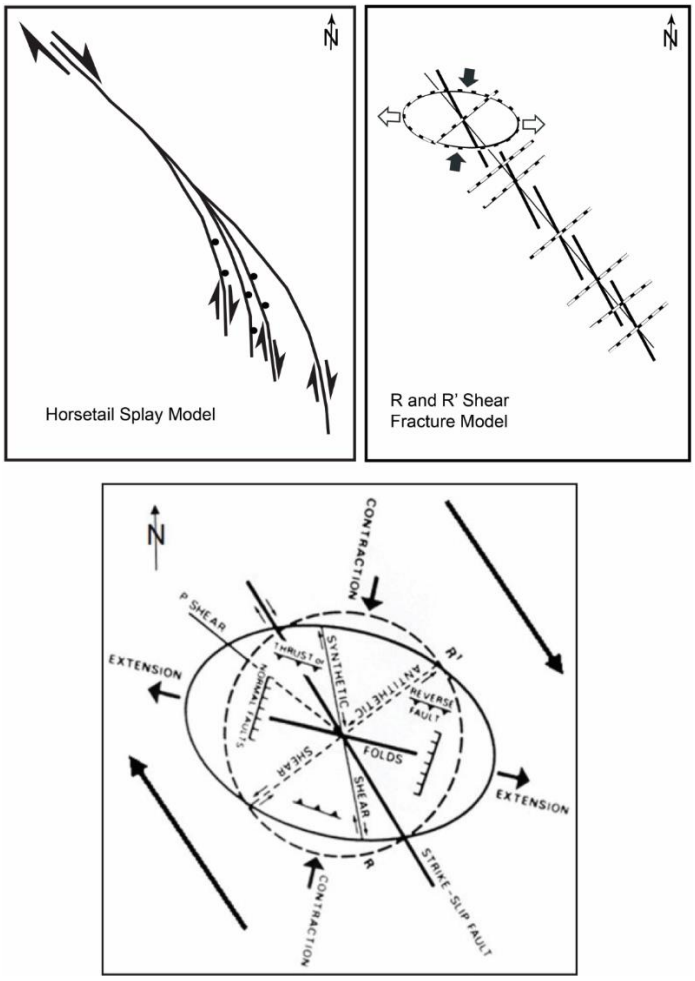

Figure 13. Various tectonic models showing the development of faults within a right lateral shear zone.